Hindawi Publishing Corporation
Journal of Nanoscience
Volume 2014, Article ID 905404, 8 pages
http://dx.doi.org/10.1155/2014/905404

Research Article

Biosynthesis and Characterization of Gold and Silver Nanoparticles Using Milk Thistle (*Silybum marianum*) Seed Extract

R. Gopalakrishnan and K. Raghu

Department of Physics, Annamalai University, Annamalainagar, Tamil Nadu 608 002, India

Correspondence should be addressed to K. Raghu; raghuk.phy@gmail.com

Received 26 November 2013; Accepted 18 January 2014; Published 12 March 2014

Academic Editor: Liqiang Jing

Biogenic synthesis of gold and silver nanoparticles from aqueous solutions using milk thistle (*Silybum marianum*) seed extract as reducing and stabilizing agent has been reported. Formation and stabilization of nanoparticles were monitored using surface plasmon resonance (SPR) bands of UV-Vis spectroscopy. Morphology of gold and silver nanoparticles was investigated using X-ray diffraction, high-resolution transmission electron microscopy with selected area electron diffraction analysis, and dynamic light scattering. Fourier transform-infrared spectroscopy was employed to identify the possible biomolecules responsible for the reduction and stabilization of nanoparticles.

1. Introduction

Metallic nanoparticles have been considered as an important area of research due to their unique and tunable physicochemical properties and biological activities as compared to their bulk counterparts. In recent years, a numerous techniques such as physical vapour deposition, chemical vapour deposition, sol-gel synthesis, microwave assisted synthesis, ultrasonication, electrochemical synthesis, precipitation method, and biosynthesis have been reported for the synthesis of metallic nanoparticles [1–11]. Biosynthesis of metallic nanoparticles by using biological organisms and plant extract is an ecofriendly alternative to those involving toxic and hazardous chemicals [12–14]. Owing to their nontoxicity, the biosynthesized nanoparticles are widely used in medicinal applications [15, 16].

Noble metals like gold and silver have been familiar since ancient times owing to their ornamental and medicinal applications. These metallic nanostructures are reported to have their potential applications in anticancer drug delivery [17], catalysis, sensors [18], wound dressing [19], medical imaging [20], and antibacterial activity [21]. The application of noble metal nanoparticles based chemistry for drinking water purification has been reported for different types of contaminants recently [22].

In continuation of several reports for the biosynthesis of gold and silver nanoparticles [23–27], recently synthesis of silver nanoparticles using *Silybum marianum* seed extract and their characterization have been reported [28]. Here, we present a green and rapid synthesis of stable gold and silver nanoparticles using milk thistle (*Silybum marianum*) seed extract as reducing and stabilizing agent. Milk thistle (SM) is a plant of the Asteraceae family bearing purple flowers and pale green leaves with some mallow thorn. Extract from the seeds of SM contains 65–80% silymarin a (Flavonolignan complex), 20–25% of fatty acids, small amount of flavonoids (taxifolin), and other polyphenolic compounds [29]. The major bioreactive constituents in SM are flavonolignans including silybin A, silyibin B, isosilybin A, isosilybin B, silydianin, and silychristin [30].

Over two thousand years, various preparations of the plant, especially the fruits, have been used medicinally to treat liver disorders [31]. SM plays a role in displacing toxins binding to the liver and causing the liver cells to

regenerate at a faster rate. Traditionally, milk thistle is used for liver cirrhosis, alcoholic hepatitis, alcoholic fatty liver, liver poisoning, and viral hepatitis. Standardized extracts from seeds of SM have been employed for the treatment of various diseases in humans, mainly liver-related disorders among those with different etiologies [32]. It has also been shown that silymarin may also be beneficial for reducing the chances of developing certain cancers [33]. The topical administration of silymarin ointments in the concentrations of 5, 10, and 20% was effective in the treatment of diabetic wounds [34]. The use of silymarin in combination with sunscreens or skincare lotions may provide an effective strategy for mitigating the adverse biological effects of solar UV radiation protecting the skin from various skin diseases caused by excessive sun exposure [35].

In this present work, we have reported an ecofriendly and rapid biosynthesis of gold and silver nanoparticles using the milk thistle (SM) seed extract and the characterization of the synthesized nanoparticles using UV-Vis spectroscopy, X-ray diffraction analysis (XRD), high-resolution transmission electron microscopy (HR-TEM), dynamic light scattering (DLS), and Fourier transform-infrared spectroscopy (FT-IR).

2. Experimental Section

2.1. Materials. All chemicals used in this investigation were of reagent grade and used as received. Hydrogen tetrachloroaurate (III) trihydrate ($HAuCl_4{\cdot}3H_2O$, 99.9%) and silver nitrate ($AgNO_3$, 99.9%) were purchased from Hi Media Laboratories Pvt. Ltd., (Mumbai, India). Deionized water was used as solvent throughout the experiment. All glassware were properly washed with tap water, rinsed several times with distilled water, and dried in oven before use. Fresh seeds of milk thistle were collected from Ootacamund, Tamil Nadu (India) and the surrounding area.

2.2. Preparation of Seed Extract. Milk thistle seeds were washed thoroughly and rinsed with deionized water and dried in hot-air oven for 3 hours at 60°C. Dried seeds were ground by using an ordinary coffee grinder to a fine powder. 5 grams of powdered seeds was mixed with 100 mL of distilled water and boiled for 5 minutes. The extract was then cooled to room temperature and filtered by Whatman filter paper (no. 1). This filtered extract can be used for over a week time.

2.3. Synthesis of Gold Nanoparticles (GNPs). 2 mL of the extract was added to 50 mL of $HAuCl_4{\cdot}3H_2O$ (10^{-4} M) aqueous solution. After 15 minutes, the color of the mixed solution (G1) turned to vivid magenta indicating the formation of GNPs. Two more samples, namely, G2 and G3, were also prepared by varying the extract volume of 4 mL and 6 mL, respectively.

2.4. Synthesis of Silver Nanoparticles (SNPs). 3 mL of the extract was added to 50 mL aqueous solution of $AgNO_3$ (10^{-3} M). After 20 minutes, the mixed solution (S1) turned to light brownish indicating the formation of SNPs. Two more samples, namely, S2 and S3, were also prepared by varying the extract volume of 5 mL and 7 mL, respectively.

2.5. Characterization of GNPs and SNPs. Formation and stability of metallic nanoparticles were examined by recording UV-Vis absorption spectra using Shimadzu UV-1650 PC Spectrophotometer through a quartz cell with 10 mm optical path. The samples were filled in a quartz cuvette of 1 cm light-path length, and the light absorption spectra were given in reference to deionized water.

The morphology of the colloidal sample was examined using a JEOL 3010 high-resolution transmission electron microscope (HR-TEM), with ultrahigh resolution (UHR) pole piece operating at an accelerating voltage of 300 kV.

Fourier transform-infrared (FT-IR) spectra of powdered specimens were recorded by a KBr pellet method using Avatar 330 FT-IR spectrometer at a resolution of 4 cm^{-1}.

X-ray diffraction (XRD) patterns of powdered samples were obtained using XPERT-PRO Diffractometer operating at 40 kV and 30 mA with Cu Kα radiation (λ = 1.5406 Å).

The particle size determination was carried out using Malvern Zetasizer Ver. 6.32 by dynamic light scattering along with zeta potential.

3. Results and Discussion

3.1. UV-Vis Spectral Analysis. UV-Vis spectroscopy is an important technique to ascertain the development and stability of nanoparticles. Colloidal solutions of metal nanoparticles usually appear intensely colored due to the surface plasmon resonance (SPR) arising from the collective oscillation of free conduction electrons induced by interacting electromagnetic radiation [36]. UV-Vis spectra of gold and silver colloids with different extract concentrations are shown in Figures 1(a) and 1(b), respectively. GNPs have given rise to the SPR band in the wavelength range of 550–500 nm at the color of vivid magenta. For SNPs, the SPR band was observed in the range 450–400 nm at the color of brownish yellow. These reported results were coherent with earlier reported literature [37–40]. With an increase in extract concentration, GNPs exhibited a blue shift by around 10 nm. SNPs have not exhibited such a shift but their SPR bands were relatively broader than those of GNPs. This may be attributed to wider size distribution of the SNPs.

3.2. X-Ray Diffraction (XRD) Analysis. The crystalline nature of nanoparticles was confirmed by XRD analysis. Figures 2(a) and 2(b) depict XRD patterns of GNPs and SNPs, respectively. The values of the diffraction angle (2θ), d-spacing, FWHM, and Miller indices for GNPs and SNPs are compiled in Tables 1 and 2, respectively. For GNPs, the peaks at 2θ = 38.07°, 44.24°, 64.43°, and 77.35° were indexed to (1 1 1), (2 0 0), (2 2 0), and (3 1 1) sets of planes of the face centered cubic (fcc) structure (with reference to JCPDS File no. 04-0784). For SNPs, the peaks at 2θ = 38.0°, 44.21°, 64.44°, and 77.33° were indexed to (1 1 1), (2 0 0), (2 2 0), and (3 1 1) sets of lattice planes of the fcc structure (with reference to JCPDS File no. 04-0783).

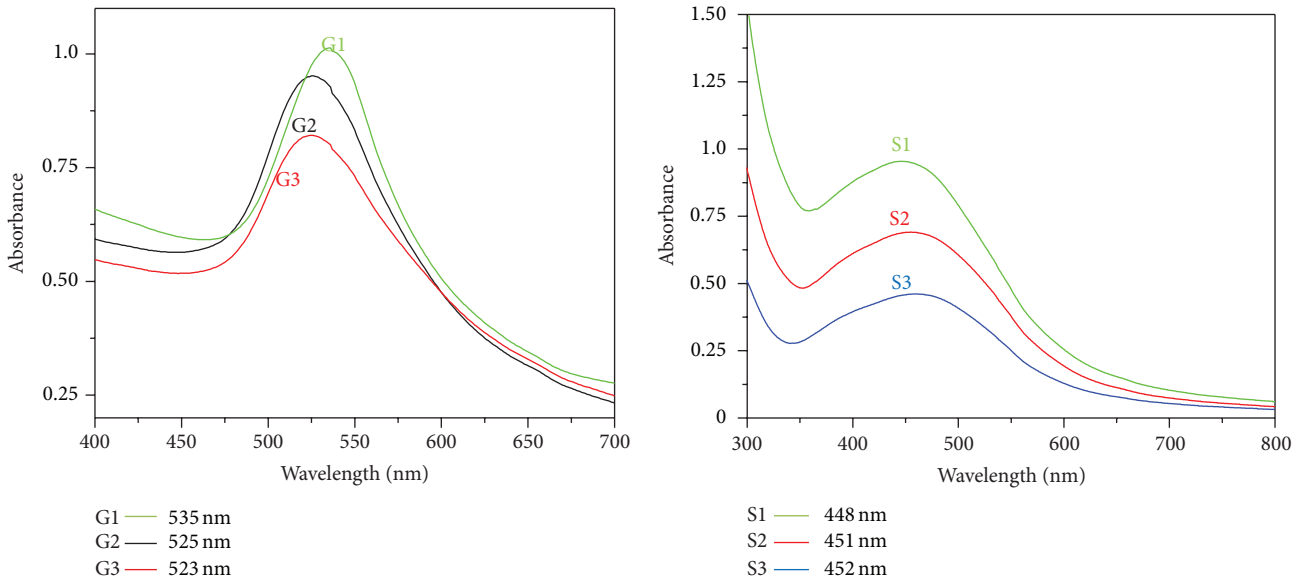

Figure 1: UV-Vis spectra of biosynthesized (a) GNPs and (b) SNPs.

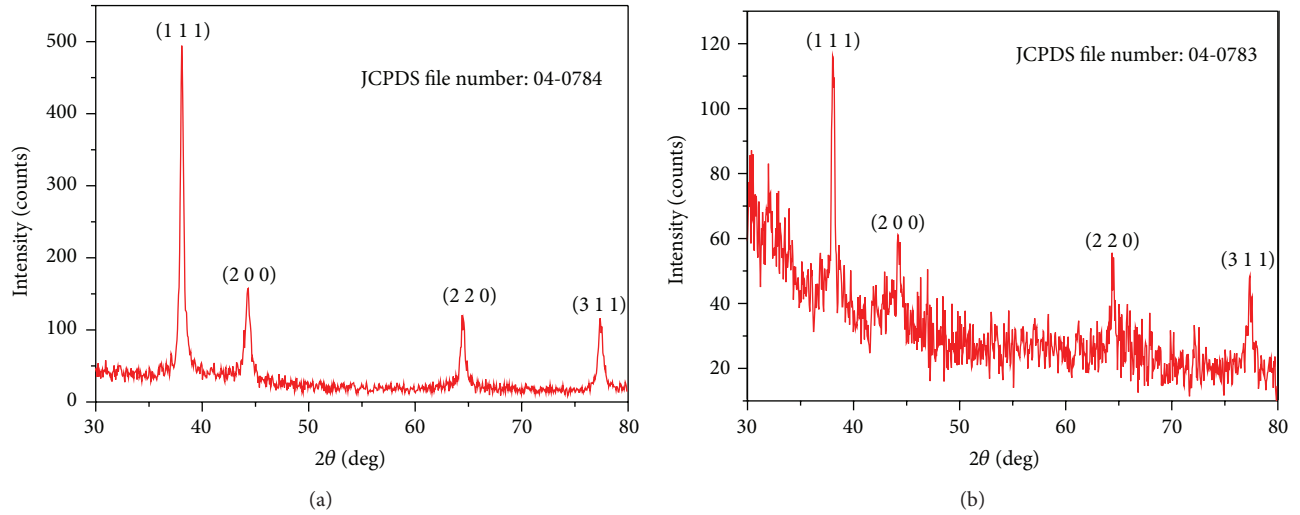

Figure 2: X-ray diffraction (XRD) pattern of (a) GNPs and (b) SNPs.

Table 1: The values of diffraction angle (2θ), d-spacing, FWHM, and Miller indices for GNPs.

Serial No.	2θ (°)	FWHM	Miller indices	d-spacing (Å)
1	38.07	0.34	(1 1 1)	2.36182
2	44.24	0.51	(2 0 0)	2.04570
3	64.43	0.54	(2 2 0)	1.44497
4	77.35	0.49	(3 1 1)	1.23268

Table 2: The values of diffraction angle (2θ), d-spacing, FWHM, and Miller indices for SNPs.

Serial No.	2θ (°)	FWHM	Miller indices	d-spacing (Å)
1	38.00	0.3	(1 1 1)	2.36359
2	44.21	0.3	(2 0 0)	2.04715
3	64.44	0.3	(2 2 0)	1.44483
4	77.33	0.13	(3 1 1)	1.23296

3.3. High-Resolution Transmission Electron Microscopic (HR-TEM) Analysis. Size and dispersion of the nanoparticles are the essential factors for the synthesized samples. The morphology of gold and silver nanoparticles was examined by HR-TEM analysis. Figures 3 and 4 depict the HR-TEM micrographs of as-synthesized metallic nanoparticles. The GNPs were predominantly spherical but some anisotropic (square shaped) particles were also seen. Differing shapes

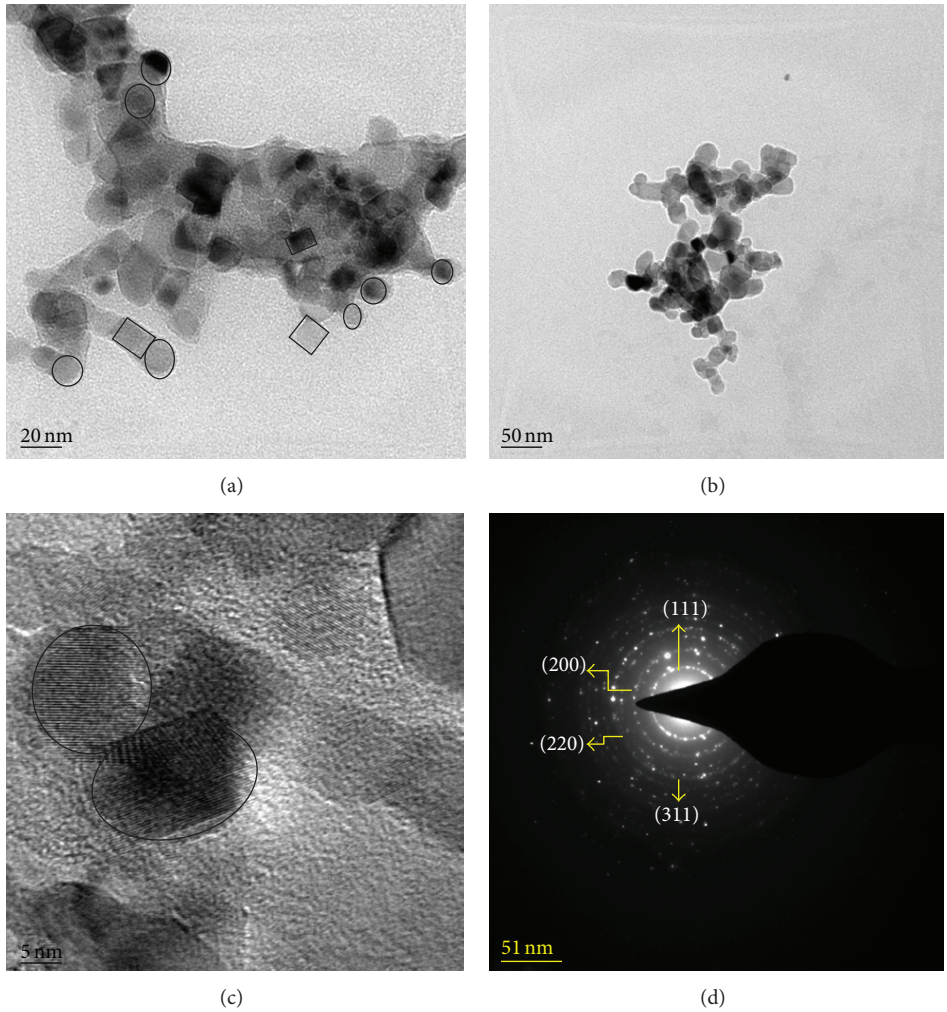

Figure 3: (a)–(d) High resolution transmission electron microscopy (HR-TEM) images of GNPs with selected area electron diffraction (SAED) pattern. Scale bars: (a) 20 nm, (b) 50 nm, and (c) 5 nm.

and sizes were due to possible aggregation of nanoparticles during storage until HR-TEM was available. SNPs were mostly spherical with wide variation in size of the particles. The nearly spherical distribution of both GNPs and SNPs has given rise to symmetric SPR bands [24]. Morphology of nanoparticles as well as their crystalline nature were again evident from selected area electron diffraction (SAED) patterns of nanoparticles (Figures 3(d) and 4(d)). Spherical morphology of the particles has been highlighted by indicators on their structure. Circular patterns of spots corresponding to reflections from (1 1 1), (2 0 0), (2 2 0) and (3 1 1) sets of lattice planes are also shown.

3.4. Dynamic Light Scattering (DLS) and Zeta Potential Analysis. DLS measures the scattering intensity based on Rayleigh scattering [41]. Particle size distribution of GNPs and SNPs is depicted in Figures 5(a) and 6(a), respectively. Size of nanoparticles varied over a wide range. The average particle size of GNPs was found to be 120 nm, while that of SNPs was around 64 nm. Zeta potential distribution for GNPs and SNPs is shown in Figures 5(b) and 6(b), respectively. Zeta potential of −15.4 for GNPs and −15.8 for SNPs exhibited moderate stability of the biosynthesized nanoparticles. Normally biosynthesized nanoparticles are reported to have absolute negative value which tends to increase with pH [21]. Earlier reports show that SNPs have zeta potential of around −15 at pH 3 [21, 42].

3.5. Fourier Transform-Infrared (FT-IR) Spectroscopic Analysis. Seeds of milk thistle contain small amounts of flavonoids and other polyphenolic compounds [29, 30]. FT-IR analyses were carried out to identify the possible biomolecules responsible for the capping and efficient stabilization of metal nanoparticles synthesized by using milk thistle seed extract. FT-IR spectra of GNPs and SNPs are shown in Figures 7(a) and 7(b), respectively. FT-IR spectrum of GNPs displays strong absorption bands at 3416 cm^{-1}, 2924 cm^{-1}, 1630 cm^{-1}, 1383 cm^{-1}, and 1031 cm^{-1} and SNPs spectrum displays strong bands at 3421 cm^{-1}, 2925 cm^{-1}, 1654 cm^{-1}, 1399 cm^{-1}, 1102 cm^{-1}, and 706 cm^{-1}. The small shifts in band positions with GNPs and SNPs suggest that the nature of coordination of capping agents on different metal surface

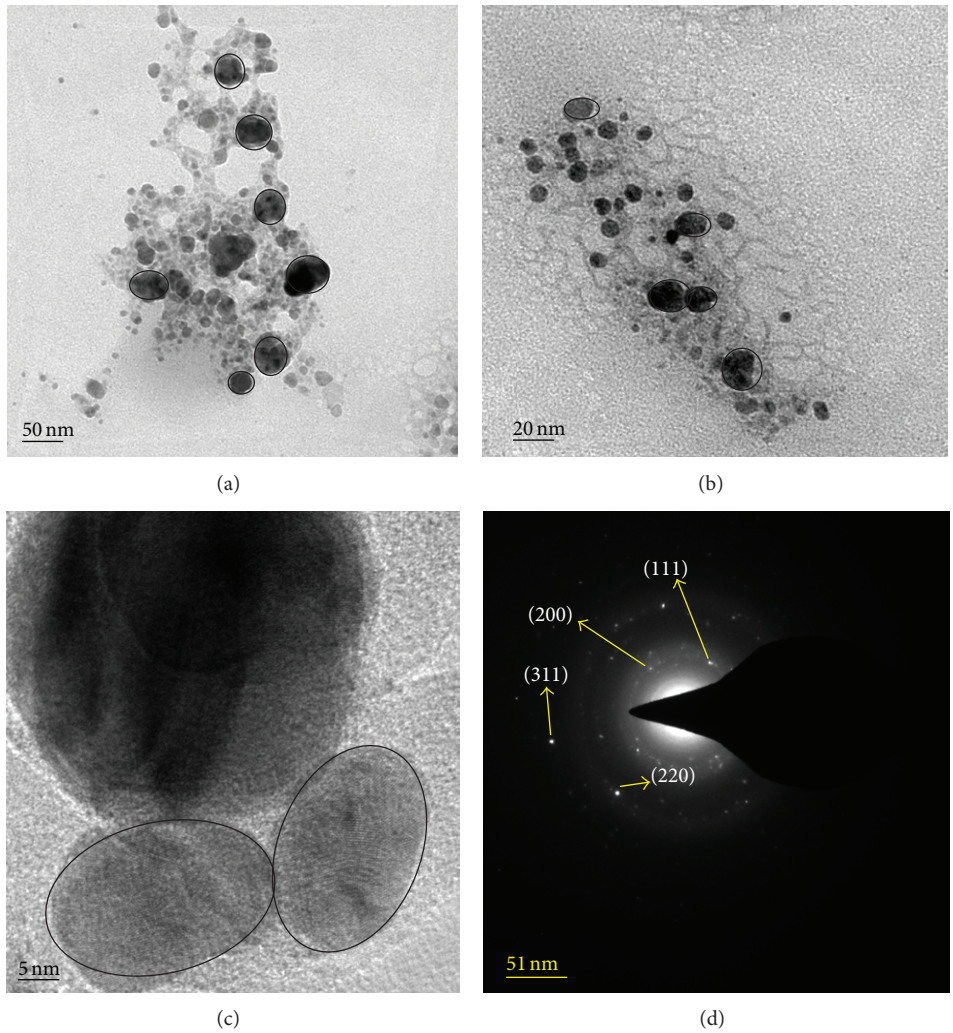

FIGURE 4: (a)–(d) High resolution transmission electron microscopy (HR-TEM) images of SNPs with SAED pattern. Scale bars: (a) 50 nm, (b) 20 nm, and (c) 5 nm.

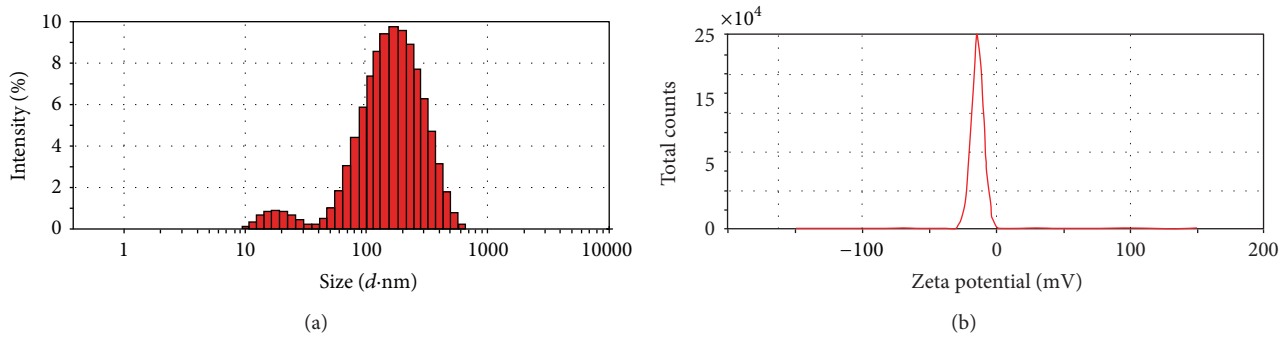

FIGURE 5: (a) Particle size distribution and (b) zeta potential distribution of GNPs by dynamic light scattering (DLS).

could be different [26]. Furthermore, the bands shift towards lower frequencies with the increasing strength of hydrogen bonding in different groups.

Strong and broad bands at 3416 cm^{-1} and 3421 cm^{-1} correspond to the stretching vibration of intermolecular hydrogen bonded O–H group in alcohols and phenols. They can also be attributed to stretching of hydrogen bonded N–H group of protein. The bands at 2924 cm^{-1} and 2925 cm^{-1} arise from C–H stretching in hydrocarbons, ethers, aldehydes, and ketones as well as O–H stretching in carboxylic acid [27]. Bands at 1630 cm^{-1} and 1654 cm^{-1} originate from N–H bending of amide-II bonds linking amino acids in protein.

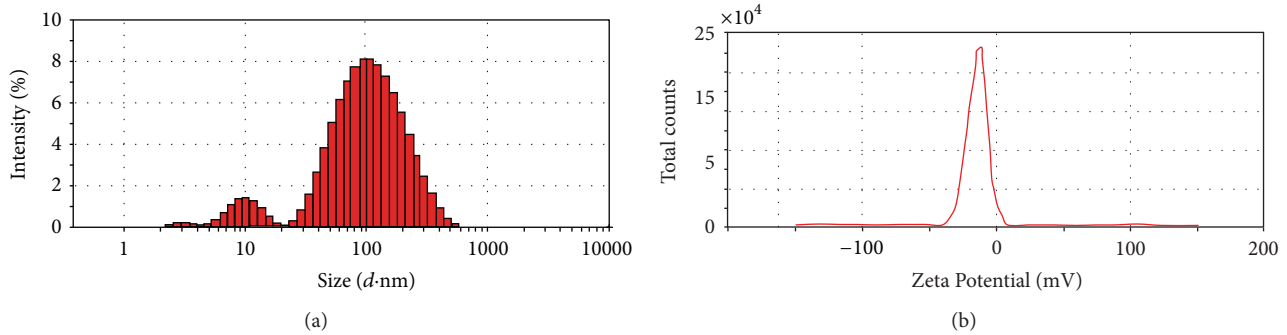

Figure 6: (a) Particle size distribution and (b) zeta potential distribution of SNPs by DLS.

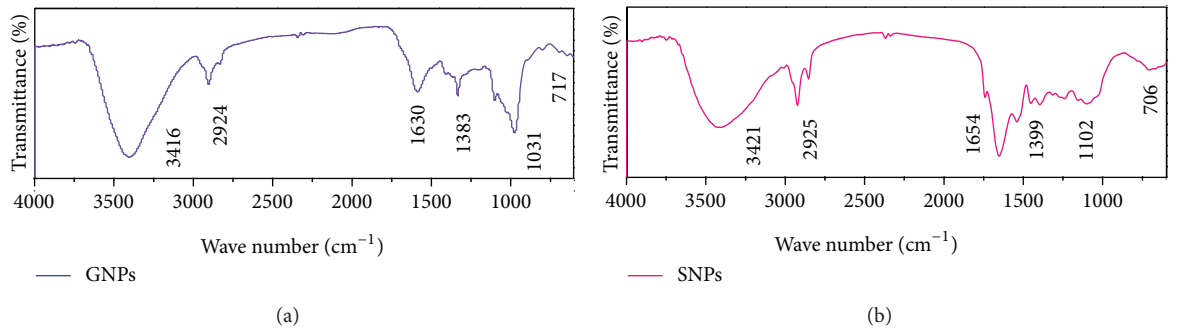

Figure 7: Fourier transform-infrared (FT-IR) spectra of biosynthesized (a) GNPs and (b) SNPs.

C=O stretching mode of carboxylic acid group as well as a C–N stretch of aromatic amines and carboxylic acids gives rise to bands at 1383 cm^{-1} and 1399 cm^{-1}. Strong bands in the region 1000–1100 cm^{-1} in both nanoparticles are assigned to C=O stretching in the ethers, alcohols, and polyphenols. C–H deformation in aromatic hydrocarbons gives rise to band at 706 cm^{-1}.

From FT-IR analysis, it was inferred that proteins and other biomolecules having functional groups of alcohols, aldehydes, carboxylic acids, and ethers bind to metal surface and also stabilize them by preventing their agglomeration. Since biomolecules are responsible for the reduction and stabilization, the biosynthesized nanoparticles are environmentally benign and nontoxic [43].

4. Conclusions

We have successfully synthesized gold and silver nanoparticles by using milk thistle (SM) seed extract as reducing and stabilizing agent. The reaction was rapid, green, ecofriendly, and economical. Syntheses of both gold and silver nanoparticles were studied using UV-Vis spectroscopy, HR-TEM, and XRD analyses. Crystallinity and particle size distribution were confirmed with SAED patterns and DLS analysis, respectively. Biomolecules responsible for stabilizing the nanoparticles were inferred from FT-IR analysis. Being stable and nontoxic, the biosynthesized nanoparticles could have potential biological and medical applications.

Conflict of Interests

The authors declare that there is no conflict of interests regarding the publication of this paper.

Acknowledgments

The authors are grateful to Dr. R. Vijayakumar, Assistant Professor of Physics, and Miss D. Saranya, Research Scholar, Department of Physics, Annamalai University, for their guidance and help.

References

[1] D. Horwat, D. I. Zakharov, J. L. Endrino et al., "Chemistry, phase formation, and catalytic activity of thin palladium-containing oxide films synthesized by plasma-assisted physical vapor deposition," *Surface and Coatings Technology*, vol. 205, no. 2, pp. S171–S177, 2011.

[2] A. C. Dillon, A. H. Mahan, R. Deshpande et al., "Hot-wire chemical vapor synthesis for a variety of nano-materials with novel applications," *Thin Solid Films*, vol. 501, no. 1-2, pp. 216–220, 2006.

[3] V. L. Chandraboss, S. Senthilvelan, L. Natanapatham, M. Murugavelu, B. Loganathan, and B. Karthikeyan, "Photocatalytic effect of Ag and Ag/Pt doped silicate non crystalline material on methyl violet-Experimental and theoretical studies," *Journal of Non-Crystalline Solids*, vol. 368, pp. 23–28, 2013.

[4] B. Karthikeyan and B. Loganathan, "Strategic green synthesis and characterization of Au/Pt/Ag trimetallic nanocomposites," *Materials Letters*, vol. 85, pp. 53–56, 2012.

[5] B. Loganathan and B. Karthikeyan, "Au core Pd/Pt shell in trimetallic Au/Pd/Pt colloidal nanocomposites-Physicochemical characterization study," *Colloids and Surfaces A: Physicochemical and Engineering Aspects*, vol. 436, pp. 944–952, 2013.

[6] B. Karthikeyan and B. Loganathan, "Rapid green synthetic protocol for novel trimetallic nanoparticles," *Journal of Nanoparticles*, vol. 2013, Article ID 168916, 8 pages, 2013.

[7] B. Karthikeyan and B. Loganathan, "A close look of Au/Pt/Ag nanocomposites using SERS assisted with optical, electrochemical, spectral and theoretical methods," *Physica E*, vol. 49, pp. 105–110, 2013.

[8] I. A. Wani, A. Ganguly, J. Ahmed, and T. Ahmad, "Silver nanoparticles: ultrasonic wave assisted synthesis, optical characterization and surface area studies," *Materials Letters*, vol. 65, no. 3, pp. 520–522, 2011.

[9] M. Starowicz, B. Stypuła, and J. Banaś, "Electrochemical synthesis of silver nanoparticles," *Electrochemistry Communications*, vol. 8, no. 2, pp. 227–230, 2006.

[10] V. L. Chandraboss, L. Natanapatham, B. Karthikeyan, J. Kamalakkannan, S. Prabha, and S. Senthilvelan, "Effect of bismuth doping on the ZnO nanocomposite material and study of its photocatalytic activity under UV-light," *Materials Research Bulletin*, vol. 48, no. 10, pp. 3707–3712, 2013.

[11] P. Mohanpuria, N. K. Rana, and S. K. Yadav, "Biosynthesis of nanoparticles: technological concepts and future applications," *Journal of Nanoparticle Research*, vol. 10, no. 3, pp. 507–517, 2008.

[12] A. R. Binupriya, M. Sathishkumar, and S.-I. Yun, "Myco-crystallization of silver ions to nanosized particles by live and dead cell filtrates of *Aspergillus oryzae* var. viridis and its bactericidal activity toward staphylococcus aureus KCCM 12256," *Industrial and Engineering Chemistry Research*, vol. 49, no. 2, pp. 852–858, 2010.

[13] K. Sneha, M. Sathishkumar, S. Y. Lee, M. A. Bae, and Y.-S. Yun, "Biosynthesis of Au nanoparticles using cumin seed powder extract," *Journal of Nanoscience and Nanotechnology*, vol. 11, no. 2, pp. 1811–1814, 2011.

[14] M. Sathishkumar, K. Sneha, and Y.-S. Yun, "Palladium nanocrystal synthesis using *Curcuma longa* tuber extract," *International Journal of Materials Sciences*, vol. 4, no. 1, pp. 11–17, 2009.

[15] M. Sathishkumar, K. Sneha, and Y.-S. Yun, "Immobilization of silver nanoparticles synthesized using *Curcuma longa* tuber powder and extract on cotton cloth for bactericidal activity," *Bioresource Technology*, vol. 101, no. 20, pp. 7958–7965, 2010.

[16] A. R. Binupriya, M. Sathishkumar, K. Vijayaraghavan, and S.-I. Yun, "Bioreduction of trivalent aurum to nano-crystalline gold particles by active and inactive cells and cell-free extract of *Aspergillus oryzae* var. viridis," *Journal of Hazardous Materials*, vol. 177, no. 1–3, pp. 539–545, 2010.

[17] S. D. Brown, P. Nativo, J.-A. Smith et al., "Gold nanoparticles for the improved anticancer drug delivery of the active component of oxaliplatin," *Journal of the American Chemical Society*, vol. 132, no. 13, pp. 4678–4684, 2010.

[18] S. Manivannan and R. Ramaraj, "Polymer-embedded gold and gold/silver nanoparticle-modified electrodes and their applications in catalysis and sensors," *Pure and Applied Chemistry*, vol. 83, no. 11, pp. 2041–2053, 2011.

[19] D. J. Leaper, "Silver dressings: their role in wound management," *International Wound Journal*, vol. 3, no. 4, pp. 282–311, 2006.

[20] M. S. Muthu and B. Wilson, "Multifunctional radionanomedicine: a novel nanoplatform for cancer imaging and therapy," *Nanomedicine*, vol. 5, no. 2, pp. 169–171, 2010.

[21] M. Sathishkumar, K. Sneha, S. W. Won, C.-W. Cho, S. Kim, and Y.-S. Yun, "Cinnamon zeylanicum bark extract and powder mediated green synthesis of nano-crystalline silver particles and its bactericidal activity," *Colloids and Surfaces B: Biointerfaces*, vol. 73, no. 2, pp. 332–338, 2009.

[22] T. Pradeep and A. Anshup, "Noble metal nanoparticles for water purification: a critical review," *Thin Solid Films*, vol. 517, no. 24, pp. 6441–6478, 2009.

[23] N. A. Begum, S. Mondal, S. Basu, R. A. Laskar, and D. Mandal, "Biogenic synthesis of Au and Ag nanoparticles using aqueous solutions of Black Tea leaf extracts," *Colloids and Surfaces B: Biointerfaces*, vol. 71, no. 1, pp. 113–118, 2009.

[24] D. Philip and C. Unni, "Extracellular biosynthesis of gold and silver nanoparticles using Krishna tulsi (*Ocimum sanctum*) leaf," *Physica E*, vol. 43, no. 7, pp. 1318–1322, 2011.

[25] G. Zhang, M. Du, Q. Li et al., "Green synthesis of Au-Ag alloy nanoparticles using cacumen platycladi extract," *RSC Advances*, vol. 3, pp. 1878–1884, 2013.

[26] D. Philip, "Biosynthesis of Au, Ag and Au-Ag nanoparticles using edible mushroom extract," *Spectrochimica Acta A*, vol. 73, no. 2, pp. 374–381, 2009.

[27] K. Mallikarjuna, G. Narasimha, G. R. Dillip et al., "Green synthesis of silver nanoparticles using Ocimum leaf extract and their characterization," *Digest Journal of Nanomaterials and Biostructures*, vol. 6, no. 1, pp. 181–186, 2011.

[28] R. Mohammadinejad, Sh. Pourseyedi, A. Baghizadeh, Sh. Ranjbar, and G. A. Mansoori, "Synthesis of silver nanoparticles using *Silybum marianum* seed extract," *International Journal of Nanoscience and Nanotechnology*, vol. 9, no. 4, pp. 221–226, 2013.

[29] K. Ramasamy and R. Agarwal, "Multitargeted therapy of cancer by silymarin," *Cancer Letters*, vol. 269, no. 2, pp. 352–362, 2008.

[30] Y. Zhao, B. Chen, and S. Yao, "Simultaneous determination of abietane-type diterpenes, flavonolignans and phenolic compounds in compound preparations of *Silybum marianum* and *Salvia miltiorrhiza* by HPLC-DAD-ESI MS," *Journal of Pharmaceutical and Biomedical Analysis*, vol. 38, no. 3, pp. 564–570, 2005.

[31] K. Flora, M. Hahn, H. Rosen, and K. Benner, "Milk thistle (*Silybum marianum*) for the therapy of liver disease," *American Journal of Gastroenterology*, vol. 93, no. 2, pp. 139–143, 1998.

[32] L. P. Ardelean, C. Mihali, A. Gavril et al., "Pharmacology of *Silybum marianum* and its active constituents. Therapeutic activity-Part 1," *Jurnal Medical Aradean*, vol. 14, no. 2, pp. 25–33, 2011.

[33] N. Bhatia, J. Zhao, D. M. Wolf, and R. Agarwal, "Inhibition of human carcinoma cell growth and DNA synthesis by silibinin, an active constituent of milk thistle: comparison with silymarin," *Cancer Letters*, vol. 147, no. 1-2, pp. 77–84, 1999.

[34] A. Aliabadi, A. Yousefi, A. Mahjoor, and M. Farahmed, "Evaluation of wound healing activity of silymarin (*Silybum marianum*)," *Journal of Animal and Veterinary Advances*, vol. 10, no. 24, pp. 3287–3292, 2011.

[35] V. Mudit and S. K. Katiyar, "Molecular mechanisms of inhibition of photocarcinogenesis by silymarin, a phytochemical from milk thistle (*Silybum marianum* L. Gaertn.) (Review)," *International Journal of Oncology*, vol. 36, no. 5, pp. 1053–1060, 2010.

[36] M. A. Noginov, G. Zhu, M. Bahoura et al., "The effect of gain and absorption on surface plasmons in metal nanoparticles," *Applied Physics B*, vol. 86, no. 3, pp. 455–460, 2007.

[37] A. R. Binupriya, M. Sathishkumar, and S.-I. Yun, "Biocrystallization of silver and gold ions by inactive cell filtrate of Rhizopus stolonifer," *Colloids and Surfaces B: Biointerfaces*, vol. 79, no. 2, pp. 531–534, 2010.

[38] K. Sneha, M. Sathishkumar, J. Mao, I. S. Kwak, and Y.-S. Yun, "Corynebacterium glutamicum-mediated crystallization of silver ions through sorption and reduction processes," *Chemical Engineering Journal*, vol. 162, no. 3, pp. 989–996, 2010.

[39] M. Sathishkumar, A. Mahadevan, K. Vijayaraghavan, S. Pavagadhi, and R. Balasubramanian, "Green recovery of gold through biosorption, biocrystallization, and pyro-crystallization," *Industrial and Engineering Chemistry Research*, vol. 49, no. 16, pp. 7129–7135, 2010.

[40] K. Sneha, M. Sathishkumar, S. Kim, and Y.-S. Yun, "Counter ions and temperature incorporated tailoring of biogenic gold nanoparticles," *Process Biochemistry*, vol. 45, no. 9, pp. 1450–1458, 2010.

[41] D. Mahl, J. Diendorf, W. Meyer-Zaika, and M. Epple, "Possibilities and limitations of different analytical methods for the size determination of a bimodal dispersion of metallic nanoparticles," *Colloids and Surfaces A: Physicochemical and Engineering Aspects*, vol. 377, no. 1–3, pp. 386–392, 2011.

[42] Z. Sadowski, I. H. Maliszewska, B. Grochowalska, I. Polowczyk, and T. Koźlecki, "Synthesis of silver nanoparticles using microorganisms," *Materials Science Poland*, vol. 26, no. 2, pp. 419–424, 2008.

[43] M. Sathishkumar, K. Sneha, and Y.-S. Yun, "Green fabrication of zirconia nano-chains using novel *Curcuma longa* tuber extract," *Materials Letters*, vol. 98, pp. 242–245, 2013.